Pediatr Radiol (2015) 45 (Suppl 3):S413–S419
DOI 10.1007/s00247-015-3425-6

Congenital spine anomalies: the closed spinal dysraphisms

Erin Simon Schwartz[1] · **Andrea Rossi**[2]

Received: 22 March 2015 / Revised: 31 May 2015 / Accepted: 23 June 2015

Abstract The term *congenital spinal anomalies* encompasses a wide variety of dysmorphology that occurs during early development. Familiarity with current terminology and a practical, clinico–radiologic classification system allows the radiologist to have a more complete understanding of malformations of the spine and improves accuracy of diagnosis when these entities are encountered in practice.

Keywords Anomaly · Children · Dysraphism · Magnetic resonance imaging · Spine

Introduction

Spinal dysraphism is increasingly being diagnosed prenatally, particularly with widespread use of fetal MRI. If not detected in utero, most cases present at birth or early in the first year; however others might not become symptomatic until later in childhood or even adulthood. MRI reveals the anatomical detail needed for appropriately diagnosing and classifying these disorders. Clinical, neuroradiologic and developmental features should be correlated when classifying spinal dysraphism [1].

✉ Erin Simon Schwartz
schwartzES@email.chop.edu

[1] Department of Radiology, The Children's Hospital of Philadelphia, Perelman School of Medicine, University of Pennsylvania, 34th Street and Civic Center Boulevard, Philadelphia, PA 19104-4399, USA

[2] Department of Radiology, G. Gaslini Children's Hospital, Genoa, Italy

Terminology

Open and closed spinal dysraphism

Spinal dysraphism can be divided into *open spinal dysraphism* and *closed spinal dysraphism* [1, 2]. In open spinal dysraphism, the neural tissue is externally exposed through a congenital osseous defect. This will be briefly described, for completeness, but will not be the focus of our discussion. Although the closed spinal dysraphism is skin-covered, cutaneous stigmata might indicate underlying dysraphism and are seen in up to 50% of patients [3, 4]. It should be noted that the term *spina bifida* has erroneously been used interchangeably with spinal dysraphism; however spina bifida more correctly refers only to incomplete fusion of the osseous posterior elements of the spine [5].

Placode

A segment of flat, non-neurulated embryonic neural tissue is referred to as a *placode*. Placodes are universal in open spinal dysraphism and are also associated with several forms of closed spinal dysraphisms.

Tethered cord

Tethered cord syndrome is not a malformation in and of itself, but a clinical syndrome [6, 7] that can result from myelomeningocele repair or a spinal lipoma, a tight filum terminale, caudal agenesis, or a split cord malformation. Tethered cord syndrome results from tension on the conus

medullaris causing progressive neurological deterioration. It should be noted that though the conus medullaris is usually low-lying in this syndrome, it is sometimes in a normal position. Common clinical manifestations of tethered cord syndrome include motor and sensory dysfunction, abnormal reflexes, incontinence, spastic gait and lower extremity deformities.

Classification of spinal dysraphism

The first step in the classification of spinal dysraphism is the clinical presentation. Is neural tissue exposed or does skin overlie it? That is, *the initial distinction is between open spinal dysraphism and closed spinal dysraphism* [1, 2].

Open spinal dysraphism

Open spinal dysraphism is not typically a diagnostic challenge. The myelomeningocele comprises the overwhelming majority of cases [1]. Distinguishing myelomeningocele from the less commonly encountered myelocele is based on the location of the neural placode. When the placode is pushed out of the confines of the canal and through the osseous and cutaneous defect by expansion of the subarachnoid space, the term myelomeningocele is correct. In contradistinction, when the subarachnoid space is not expanded, the placode remains in plane with or deep to the cutaneous surface, and the term myelocele should be used. More clinically relevant diagnostic concerns include the extent of any associated Chiari II malformation, any concomitant hydrocephalus, and potential complications following surgical closure [8–10].

Closed spinal dysraphism

The group of closed spinal dysraphisms is far more heterogeneous than that of open spinal dysraphisms. The clinical findings are highly relevant in guiding the differential diagnosis, particularly the presence or absence of a subcutaneous mass.

Closed spinal dysraphism without subcutaneous mass

Skin-covered lesions without a subcutaneous mass might be occult on casual inspection but a detailed examination of the spinal cutaneous tissues sometimes reveals regional hirsutism or dorsal dimples. All dermal sinuses arising above the superior margin of the gluteal cleft should be considered to be communicating with the spinal canal until proved otherwise. A tail or prominent lumbar skin tag, lower extremity abnormalities and anorectal malformations including imperforate anus frequently coexist with underlying spinal anomalies, and MRI is warranted for evaluation.

Closed spinal dysraphism with subcutaneous mass

The mass is typically over the lumbar or lumbosacral regions. Four main malformations present in this fashion: lipomyelocele, lipomyelomeningocele, meningocele and terminal myelocystocele [1, 2]. In lipoma with dorsal defect (lipomyelocele and lipomyelomeningocele), a subcutaneous lipoma creates the clinically evident mass.

Lipoma with dural defect

Lipomyeloceles and lipomyelomeningoceles present with a lumbar subcutaneous fat-containing mass, typically beginning cephalad to the gluteal cleft and extending caudally, often in an asymmetrical fashion [11]. They frequently grow along with any increase in general fat deposition during childhood [12].

In the lipomyelocele (also known as lipomyeloschisis) the interface of the placode and the lipoma is within the spinal canal, with continuity of the intraspinal lipoma and the overlying fat through the posterior osseous defect (Fig. 1). In contrast, with the lipomyelomeningocele, the interface of the placode and the lipoma is positioned posterior to the posterior margin of the spinal canal because of dilatation of the subarachnoid space (Fig. 2). Usually, the placode-lipoma interface is obliquely positioned, with the placode being elongated and rotated with the lipoma unilaterally, and the meninges herniating out contralaterally [2].

The meningocele is a protruding cerebrospinal fluid (CSF)-filled sac, which is lined by both pachymeninges and leptomeninges, through a posterior osseous defect. Most are lumbar or sacral. Although by definition the spinal cord itself does not enter the meningocele, the cord can be tethered at the defect. Elongated nerve roots and the filum terminale can traverse the sac, as well.

Myelocystoceles are caused by herniation of the spinal cord, which contains an expanded central canal, within a meningocele. The neurulation of the affected spinal cord levels is nearly complete except for a small placode connecting to the inner cutaneous surface (also known as a limited dorsal myeloschisis). Myelocystoceles are rare and can be terminal or nonterminal, based on the location of the malformation (e.g., involving the conus medullaris or a more proximal portion of the spinal cord, respectively).

Terminal myelocystoceles result from herniation of a large terminal syringohydromyelic cavity into a posterior meningocele via a large posterior osseous defect. They are frequently associated with the OEIS complex (omphalocele, exstrophy of the cloaca, imperforate anus and spinal anomalies) [13]. The nonterminal myelocystocele presents as a large meningocele, typically with a narrow neck traversing a small posterior osseous defect. The lesion can contain a dilated,

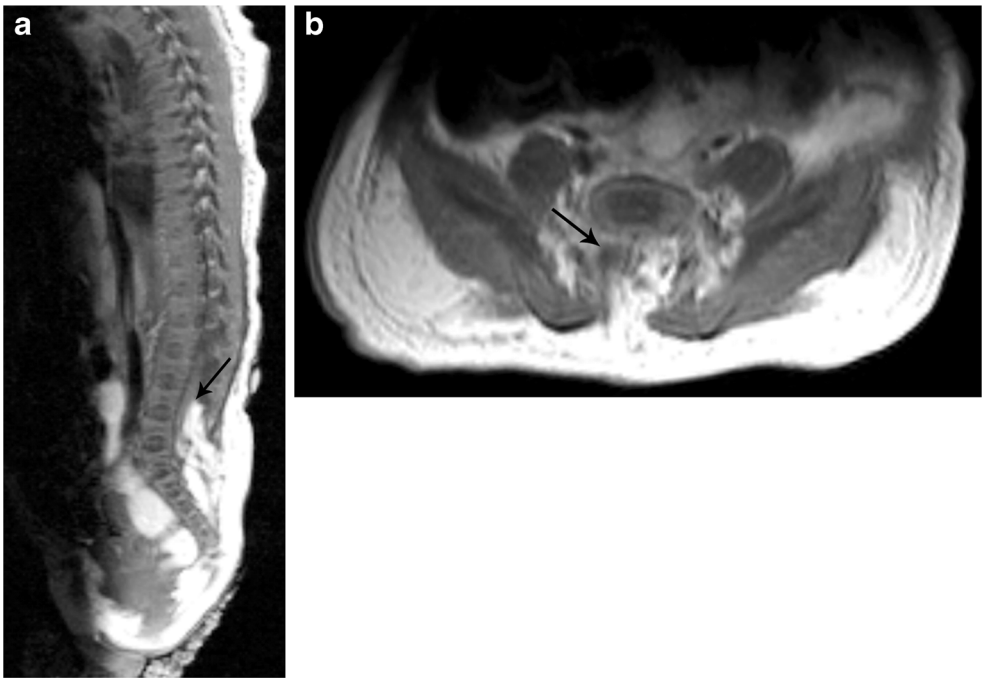

Fig. 1 Lipomyelocele in a 2-day-old boy. **a** Sagittal T1-weighted MR image of the lumbosacral spine shows the interface of the placode and the lipoma within the confines of the spinal canal (*arrow*), via a posterior osseous defect. Note the intact overlying skin in this closed spinal dysraphism. **b** Axial T1-weighted MR image at the level of the sacrum shows the subcutaneous fat asymmetrically entering the spinal canal and deviating the low-lying placode (*arrow*) to the left

CSF-filled cavity lined by the posterior wall of the spinal cord or a narrow fibroneurovascular stalk attached to the meningocele, the latter being considered by some to be an abortive form of nonterminal myelocystocele [14]. In these so-called abortive myelocystoceles a narrow stalk emanates from the posterior aspect of a relatively normal-appearing spinal cord and fans out into the posterior meningocele. In either form, the apex of the sac is covered by a thick layer of squamous epithelium, and inferior to the abnormality the spinal cord is normal. Components of the Chiari II malformation are seen in approximately 40% of nonterminal myelocystoceles [14].

Closed spinal dysraphism without subcutaneous mass

Simple dysraphic states

Often grouped clinically, these more common abnormalities are usually encountered in somewhat older children who typically present with tethered cord syndrome rather than prominent cutaneous stigmata [15, 16]. Ultrasound can be a useful tool for screening the neonate or young child with suspected spinal cord tethering, particularly those with more proximal, complex or larger (greater than 5 mm in diameter) dimples.

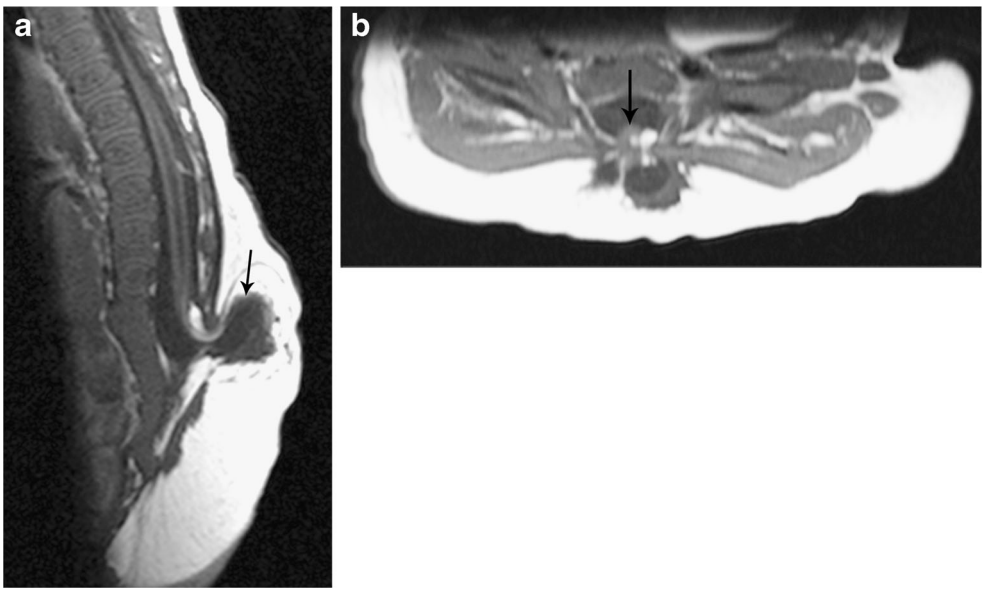

Fig. 2 Lipomyelomeningocele in a 2-month-old boy. **a** Sagittal T1-weighted MR image of the lumbosacral spine shows the placode and fat traversing a posterior osseous defect with dilated cerebrospinal space in the subcutaneous fat (*arrow*). Note the syringohydromyelia in the tethered spinal cord. **b** Axial T1-weighted MR image at the level of the sacrum shows the subcutaneous fat asymmetrically entering the spinal canal and deviating the low-lying placode (*arrow*) to the right

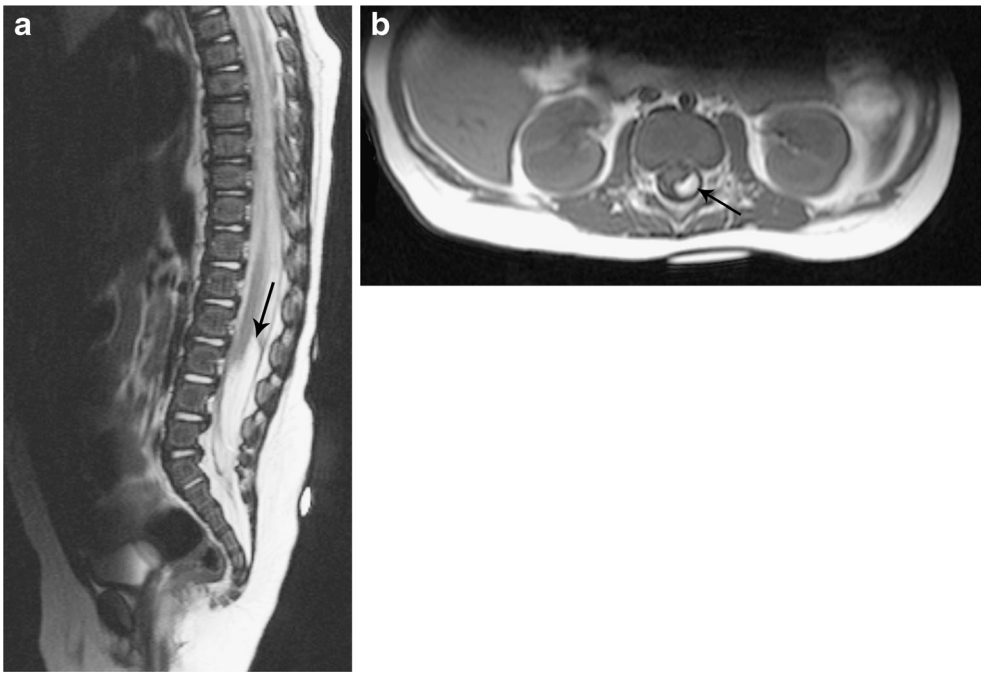

Fig. 3 Intradural lipoma in a 4-month-old boy. **a** Sagittal T2-weighted and (**b**) axial T1-weighted MR images of the lumbar spine show the intradural fatty mass tethering the spinal cord (*arrow*). Note the intact posterior elements, helping to distinguish the intradural lipoma from lipoma with dorsal defect

Further characterization with MRI is warranted when the spinal cord is found to be low-lying, the filum terminale is thickening or an intraspinal lesion is identified.

Intradural lipomas lie along the midline within a completely formed dural sac. They are usually lumbosacral and present with tethered cord syndrome, whereas cervicothoracic lipomas frequently present later with signs of spinal cord compression (Fig. 3).

The classic filar lipoma is caused by fibrolipomatous thickening of the filum terminale. Incidental fatty infiltration within the filum terminale is estimated to occur in 1.5–5% of normal adults [17, 18]. Therefore, some consider it to be an anatomical variant if there are no signs or symptoms of spinal cord tethering. Axial T1-weighted imaging is the most sensitive sequence for detection of fat within the filum terminale.

The tight filum terminale results from a shortened, thick filum terminale that causes tethering and impaired ascent of the conus medullaris, usually detected on axial T2-weighted images (Fig. 4). This is more frequently seen with other malformations, such as the split cord malformation or the dorsal dermal sinus [1, 2]. The termination of the conus medullaris lies below the L2 level in 86% of patients with a tight filum terminale [3]. The normal filum terminale should be less than 2 mm in diameter [19].

The dermal sinus is a tract lined by epithelium connecting the dorsal cutaneous surface to the spinal cord or its meninges. It most frequently occurs in the lumbosacral region, but even occipital sinuses are encountered [20, 21]. Often these are in association with visible cutaneous stigmata including a capillary hemangioma, hairy nevus, or hyperpigmented patches. Complications of this communication between the skin surface and the CNS include local bacterial infection, meningitis and abscess [22]. Dermal sinuses can be seen on sagittal MR sequences as a thin linear band of hypointense signal,

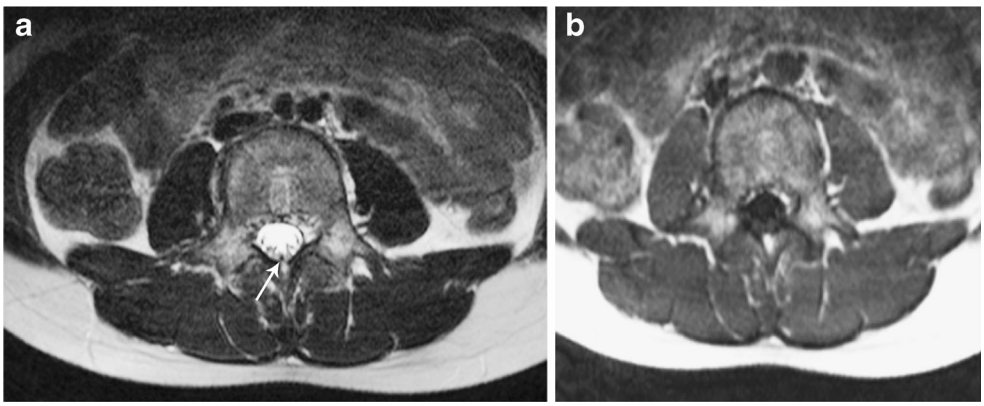

Fig. 4 Tight filum terminale in a 9-year-old boy. **a** Axial T2-weighted MR image demonstrates the thickened T2-hypointense filum terminale at the L4 level (*arrow*). **b** Axial T1-weighted MR image through the same level shows no T1 shortening to indicate fat

typically obliquely traversing the subcutaneous fat (Fig. 5). Associated spinal inclusion cysts are common and can also become infected.

The persistent terminal ventricle is a prominent intramedullary cavity within the conus medullaris, which is lined by ependyma. Enlargement and more cyst-like configuration could be an anatomical variant or the result of obstruction [23]. Differentiation from syringohydromyelia is based on location (directly above the filum terminale). The persistent terminal ventricle can be distinguished from intramedullary tumors by the completely cystic nature of the persistent terminal ventricles, including absence of contrast enhancement and stability, or even reduction in size, over time.

Complex dysraphic states

The notochord is intimately involved in the formation of the spine and spinal cord, among numerous other structures in the human body. Because the notochord is created during gastrulation, spinal dysraphism originating during this period is not surprisingly associated with multisystem anomalies. Derangement during notochordal development has been categorized into: (1) disorders of midline notochordal integration and (2) disorders of notochordal formation [1, 2]. The disorders of integration result in longitudinal spinal cord splitting; the disorders of formation cause absence of a notochordal segment and, as a result, absence of the corresponding spinal cord and spine segments.

Disorders of midline notochordal integration

Diastematomyelia (split cord malformation) refers to a splitting of the spinal cord in two [24, 25]. Failure of midline integration results in parallel notochordal processes divided by a line of primitive streak cells. Each separate process induces a separate neural plate. The resultant morphology is dependent on the primitive streak development. If the streak cells become cartilage and bone, the hemicords will be in their own dural sacs, which are separated by an osteocartilaginous spur. On the other hand, if the primitive streak cells are entirely or largely reabsorbed, the hemicords will lie within one dural tube, with or without a thin fibrous septum. This is the basis for the classification of the two forms of diastematomyelia [24]. Type I is diagnosed when each hemicord is within its own dural tube and they are separated by an extradural osseous septum extending midsagittally from the posterior aspect of the vertebral body to the posterior elements (Fig. 6) [24]. The septum might be oblique or incomplete, however. Children often present with scoliosis and spinal cord tethering; a large patch of hair overlying the upper thoracic spine is a consistent sign of an underlying diastematomyelia [1]. Associated vertebral abnormalities are the norm in type I. Generally the spur results in the spinal cord tethering because it is positioned at the caudal end of the split, just above the point of spinal cord fusion.

Type II features a single dural tube containing the hemicords [24, 25]. An intervening fibrous septum is sometimes present but is uncommon, and there might only be

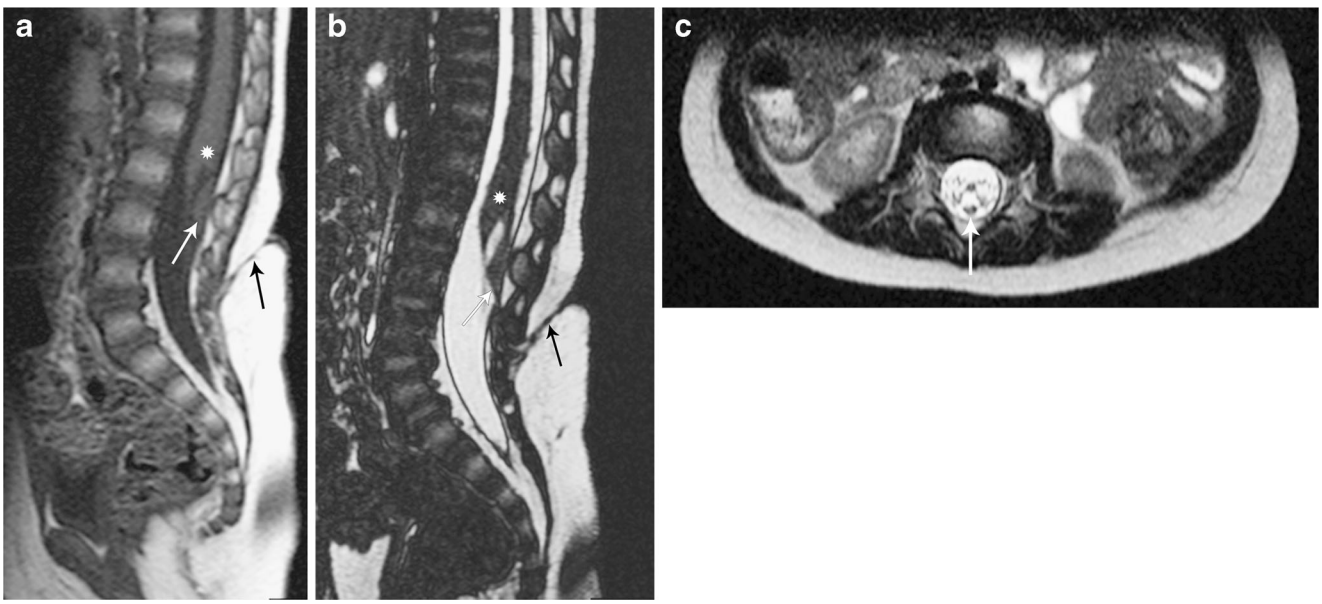

Fig. 5 Dorsal dermal sinus in a 14-month-old girl. **a–c** Sagittal T1-W (**a**) and CISS (**b**) and axial T2-weighted (**c**) MR images through the lumbar spine show the hypointense sinus obliquely traversing from the cutaneous ostium to the spinal canal (*black arrow*). An intradural spinal inclusion cyst (*white arrow*) is dorsal to the conus medullaris (*star*). *CISS* constructive interference in steady state

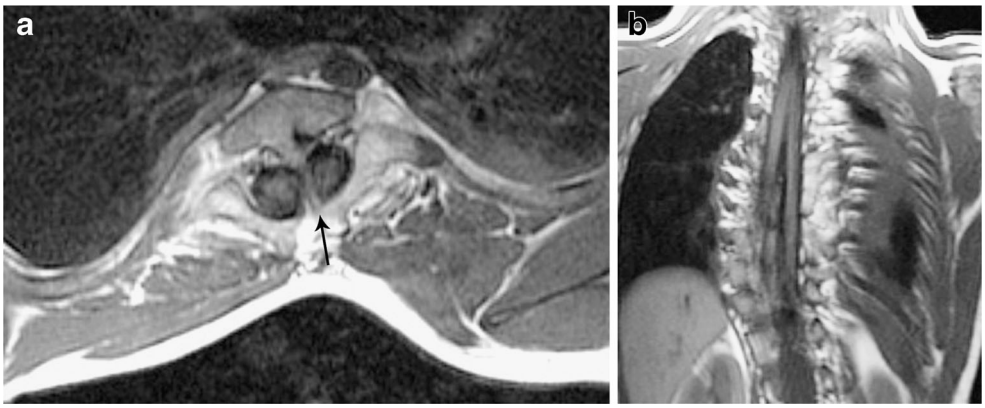

Fig. 6 Diastematomyelia type I in a 7-year-old girl. **a** Axial and (**b**) coronal T1-weighted MR images of the thoracic spine show the two discrete dural tubes separated by an osteocartilaginous septum (*arrow*)

partial spinal cord splitting [2]. Spilt cord malformation can be surprisingly challenging to appreciate on sagittal MRI [2, 26]. Orthogonal planes are required to make the diagnosis. The conus medullaris is frequently low-lying, and there is a high association with either lipomas of the filum terminale or a tight filum terminale. Vertebral anomalies are not usually associated.

Disorders of notochordal formation

Caudal agenesis, or caudal regression syndrome, includes partial or complete agenesis of the distal spinal column, imperforate anus, genitourinary anomalies, bilateral renal absence or dysplasia, pulmonary hypoplasia and lower extremity anomalies [27]. Caudal agenesis might be a component in syndromic complexes such as OEIS [22], the Currarino triad (partial sacral agenesis, anorectal malformations and presacral teratoma or meningocele) [28–30] and VACTERL (vertebral anomalies, imperforate anus, cardiac malformations, tracheoesophageal fistula, renal anomalies and limb deformities) [14]. The vertebral anomalies range from absence of coccygeal segments to agenesis from the lower thoracic spinal levels inferiorly; the majority affect only the sacrum and coccyx.

Caudal agenesis has been divided into two forms, dependent on the termination and morphology of the conus medullaris: the high and abruptly terminating (type I) or the low and tethered (type II). The degree of spinal cord dysplasia correlates with the severity of the spinal malformation, with the type I being more severe [31]. In type I, the degree of vertebral involvement ranges from absence of sacral segments below S2 as well as the coccyx, to agenesis of all lower thoracic, lumbar, sacral and coccygeal vertebrae, although the lowest intact vertebra is usually between L5 and S2 (Fig. 7). Associated aplasia of the caudal metameres of the developing spinal cord results in the characteristic abrupt spinal cord termination with a hatchet or wedge shape [32–34]. The spinal cord might terminate high. The thecal sac also tapers below the conus termination and ends at an unusually high level (above S2). In type II caudal agenesis, vertebral dysgenesis is less severe, with only the lowermost sacral or coccygeal segments absent. Only the very tip of the conus medullaris is absent, affecting only those metameres formed by secondary neurulation. This partial absence of the conus medullaris can be subtle or challenging to detect because of the caudal stretching of the conus and tethering by a tight filum, lipomyelomeningocele, lipoma, terminal myelocystocele or

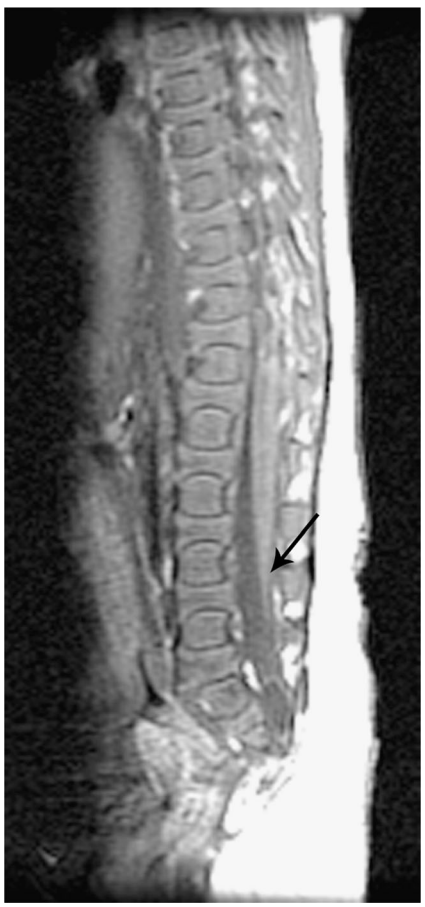

Fig. 7 Caudal agenesis in a 6-week-old girl. Sagittal T1-weighted MR image of the lower spine shows absence of much of the first sacral segment as well as the remainder of the sacrum and coccyx. The spinal cord is elongated, low-lying, and tethered (*arrow*)

anterior sacral meningocele. Unlike with type I, these children typically present with spinal cord tethering.

Segmental spinal dysgenesis includes segmental agenesis or dysgenesis of the lower spine, with a concordant segmental abnormality of the spinal cord and nerve roots, congenital lower extremity weakness or paralysis and deformities [34]. This could involve any of the lower thoracic, lumbar or sacral segments of the spine. In the most extreme cases, the spinal cord at the affected level is absent and the vertebral body is focally aplastic, resulting in an acute kyphosis. Below a more normal-appearing proximal segment, the canal is extremely narrow or even absent. The lower spinal cord segment is typically thick and abnormally low [34]. Horseshoe kidney is commonly associated and located in the concavity of the kyphosis [2].

Conclusion

The morphology of closed spinal dysraphisms can seem quite complex. However, a systematic approach correlating clinical, embryological and neuroimaging data greatly facilitates accurate diagnoses. Application of this approach will improve diagnosis and increase the quantity and quality of information in the radiologic reports concerning these entities.

Conflicts of interest The authors have no financial interests, investigational or off-label uses to disclose.

References

1. Tortori-Donati P, Rossi A, Cama A (2000) Spinal dysraphism: a review of neuroradiological features with embryological correlations and proposal for a new classification. Neuroradiology 42: 471–491
2. Rossi A, Gandolfo C, Morana G et al (2006) Current classification and imaging of congenital spinal abnormalities. Semin Roentgenol 41:250–273
3. Warder DE (2001) Tethered cord syndrome and occult spinal dysraphism. Neurosurg Focus 10, e1
4. Drolet B (1998) Birthmarks to worry about. Cutaneous markers of dysraphism. Dermatol Clin 16:447–453
5. French BN (1983) The embryology of spinal dysraphism. Clin Neurosurg 30:295–340
6. Warder DE, Oakes WJ (1993) Tethered cord syndrome and the conus in a normal position. Neurosurgery 33:374–378
7. Warder DE, Oakes WJ (1994) Tethered cord syndrome: the low-lying and normally positioned conus. Neurosurgery 34:597–600
8. Herman JM, McLone DG, Storrs BB et al (1993) Analysis of 153 patients with myelomeningocele or spinal lipoma reoperated upon for a tethered cord. Pediatr Neurosurg 19:243–249
9. McLone DG, Dias MS (1991) Complications of myelomeningocele closure. Pediatr Neurosurg 17:267–273
10. Scott RM, Wolpert SM, Bartoshesky LF et al (1986) Dermoid tumors occurring at the site of previous myelomeningocele repair. J Neurosurg 65:779–783
11. Naidich TP, McLone DG, Mutleur S (1983) A new understanding of dorsal dysraphism with lipoma (lipomyeloschisis): radiological evaluation and surgical correction. AJNR Am J Neuroradiol 4:103–116
12. Knittle JL, Timmers K, Ginsberg-Fellner F et al (1979) The growth of adipose tissue in children and adolescents. Cross-sectional and longitudinal studies of adipose cell number and size. J Clin Invest 63:239–246
13. Smith NM, Chambers HM, Furness ME et al (1992) The OEIS complex omphalocele-exstrophy-imperforate anus-spinal defects: recurrence in sibs. J Med Genet 29:730–732
14. Rossi A, Piatelli G, Gandolfo C et al (2006) Spectrum of nonterminal myelocystoceles. Neurosurgery 58:509–515
15. Tortori-Donati P, Cama A, Rosa ML et al (1990) Occult spinal dysraphism: neuroradiological study. Neuroradiology 31:512–522
16. Raghavan N, Barkovich AJ, Edwards M et al (1989) MR imaging in the tethered spinal cord syndrome. AJNR Am J Neuroradiol 10: 27–36
17. Brown E, Matthes JC, Bazan C 3rd et al (1994) Prevalence of incidental intraspinal lipoma of the lumbosacral spine as determined by MRI. Spine 19:833–836
18. Uchino A, Mori T, Ohno M (1991) Thickened fatty filum terminale: MR imaging. Neuroradiology 33:331–333
19. Yundt KD, Park TS, Kaufman BA (1997) Normal diameter of filum terminale in children: in vivo measurement. Pediatr Neurosurg 27: 257–259
20. Scotti G, Harwood-Nash DC (1980) Congenital thoracic dermal sinus: diagnosis by computer assisted metrizamide myelography. J Comput Assist Tomogr 4:675–677
21. Barkovich AJ, Edwards MS, Cogen PH (1991) MR evaluation of spinal dermal sinus tracts in children. AJNR Am J Neuroradiol 12: 123–129
22. Elton S, Oakes WJ (2001) Dermal sinus tracts of the spine. Neurosurg Focus 10, e4
23. Coleman LT, Zimmerman RA, Rorke LB (1985) Ventriculus terminalis of the conus medullaris: MR findings in children. AJNR Am J Neuroradiol 16:1421–1426
24. Pang D, Dias MS, Ahab-Barmada M (1992) Split cord malformation. Part I: a unified theory of embryogenesis for double spinal cord malformations. Neurosurgery 31:451–480
25. Pang D (1992) Split cord malformation. Part II: clinical syndrome. Neurosurgery 31:481–500
26. Tortori-Donati P, Rossi A, Biancheri R et al (2005) Congenital malformations of the spine and spinal cord. In: Tortori-Donati P (ed) Pediatric neuroradiology. Springer, Berlin, pp 1551–1608
27. Duhamel B (1961) From the mermaid to anal imperforation: the syndrome of caudal regression. Arch Dis Child 36:152–155
28. Currarino G, Coln D, Votteler T (1981) Triad of anorectal, sacral, and presacral anomalies. AJR Am J Roentgenol 137:395–398
29. Dias MS, Azizkhan RG (1998) A novel embryogenetic mechanism for Currarino's triad: inadequate dorsoventral separation of the caudal eminence from hindgut endoderm. Pediatr Neurosurg 28:223–229
30. Gudinchet F, Maeder P, Laurent T et al (1997) Magnetic resonance detection of myelodysplasia in children with Currarino triad. Pediatr Radiol 27:903–907
31. Nievelstein RAJ, Valk J, Smit LME et al (1994) MR of the caudal regression syndrome: embryologic implications. AJNR Am J Neuroradiol 15:1021–1029
32. Pang D (1993) Sacral agenesis and caudal spinal cord malformations. Neurosurgery 32:755–779
33. Barkovich AJ, Raghavan N, Chuang SH (1989) MR of lumbosacral agenesis. AJNR Am J Neuroradiol 10:1223–1231
34. Tortori-Donati P, Fondelli MP, Rossi A et al (1999) Segmental spinal dysgenesis. Neuroradiologic findings with clinical and embryologic correlation. AJNR Am J Neuroradiol 20:445–456